IRSTI 31.17.15

[1,2*]G. Xanthopoulou and [1]G. Vekinis

[1]Institute of Materials Science, NCSR "Demokritos", Aghia Paraskevi, 15310, Greece
[2]Department of Theory of Aircraft Engines, Samara National Research University, 34 Moskovskoe shosse, 443086 Samara, Russia
[*]e-mail: gxantho@ims.demokritos.gr

Self-propagating high-temperature synthesis of nial intermetallic compounds

Abstract. In this work, the self-propagating high-temperature synthesis (SHS) method was utilized for the synthesis of the B2 NiAl compound. Elemental nickel and aluminum powders were mixed, die-pressed, and pre-heated in a furnace in which the SHS reaction was initiated and propagated. The influence of pre-heating temperature was evaluated against the final composition, phase formation, microstructure and hardness of the final compact. Conditions were found under which, the final product forms through solidification from the melt and (irrespective of the furnace temperature) consists only of the B2 NiAl. The NiAl compacts formed consisted of a core which is essentially pore free and accounts for ~80% of the total volume and a high porosity shell around it. The microstructure consists of large, equiaxial grains with linear grain boundaries indicative of high phase stability. Finally, it was found that as the pre-heating temperature increases the hardness of the NiAl compact decreases; a transient temperature analysis enabled to interpret this observation.

Practical significance of the results: NiAl is an extremely useful industrial material with many high temperature applications.

Key words: self-propagating high-temperature synthesis, NiAl

Introduction

The B2 ordered intermetallic NiAl compounds exhibit a wide range of physical and mechanical properties which show promise for applications ranging from high-pressure turbine blades to buried interconnects in electronic components [1]. NiAl forms an adherent film on oxidation in air at temperatures up to 1200°C, indicating good corrosion resistance as demonstrated by its use as a base for some protective coatings on nickel-based superalloys. The structure remains fully ordered up to the melting point, implying a resistance to diffusion-controlled processes, such as precipitation, grain growth, oxidation and creep deformation. The large phase width of NiAl suggests a potential for substitutional alloying to improve strength and oxidation resistance. NiAl is approximately 30% less dense than nickel (a common superalloy base) and has a melting point 200°C higher. On the other hand, drawbacks of this type of intermetallics include low ductility and toughness [1, 2].

Conventionally intermetallics are fabricated by processes such as vacuum arc melting and their final microstructure is refined by several thermomechanical treatments. To reduce costs and complexity, Self-Propagating High-Temperature Synthesis (SHS) and thermal explosion, has also been used [3-7]. In the SHS method, the exothermic reaction between the powder constituents is initiated and becomes self-sustaining to yield the final product progressively without requiring additional heat. Compared to conventional processing methods, the main advantages of SHS are: (i) higher purity products because of the high reaction temperature which can volatilize and hence "remove" low boiling point impurities, (ii) simplicity since there is no need for expensive processing facilities and equipment, (iii) low operating and processing costs due to the short exothermic reaction times, (iv) ability to fabricate non-equilibrium or metastable phases because of the high thermal gradients and rapid cooling rates and (v) capability for producing a wide range of inorganic materials consolidated into a final product in one step by utilizing the chemical energy of the reactants [8-10]. However, there are some disadvantages of the method such as high porosity (which may be reduced by simultane-

 Printed in Kazakhstan

ous compression [11]), microstructural inhomogeneities, etc. Several reviews of the combustion synthesis technique and its prospects have appeared in the literature [12-22].

Thermodynamics

During the combustion synthesis reaction there are four important temperatures which affect the process of the reaction and the properties of the final product: 1) the initial or preheating temperature T_o, which is the temperature of the powder compact of the reactant sample before the reaction is initiated, 2) the ignition temperature T_{ig}, which represents the point at which the SHS reaction is spontaneously activated without further external heat supply, 3) the adiabatic combustion temperature T_{ad}, which is the maximum combustion temperature achieved under adiabatic conditions and (4) the actual combustion temperature T_c, achieved normally under non-adiabatic conditions [23].

The amount of heat, H(R) required to raise the temperature of the reactants from the initial temperature T_o to the ignition temperature T_{ig} (i.e. the temperature at which the exothermic reaction initiates) is given by the following equation:

$$H(R) = \int_{T_o}^{T_{ig}} \sum n_i C_p(R_i) dT + \sum_{T_o - T_{ig}} n_i L(R_i) \quad (1)$$

where n_i, $C_p(R_i)$, and $L(R_i)$ represent the reaction stoichiometric coefficients, heat capacities and the phase transformation enthalpies (if the reactants go through a phase change such as from solid to liquid) of the reactants respectively. At a certain distance from the heat source, the reactant compact reaches steady state conditions; in this state the heat of the reaction $\Delta H(T_{ig})$ is only used to heat the adjacent layer from T_o to T_{ig}. At this point, the amount of heat available to be absorbed by the products under adiabatic conditions is, therefore, H(P), which raises the temperature from T_{ig} to the adiabatic temperature $T_{ad}(T_o)$, i.e.

$$\Delta H(T_{ig}) = -[H(R) + H(P)] \quad (2)$$

where H(P) is given by:

$$H(P) = \int_{T_{ig}}^{T_{ad}(T_o)} \sum n_j C_p(P_j) dT + \sum_{T_{ig} - T_{ad}(T_o)} n_i L(P_j) \quad (3)$$

where n_j, $C_p(P_j)$, and $L(P_j)$ represent the reaction stoichiometric coefficients, heat capacities and the phase transformation enthalpies (if the products go through a transformation phase change) of the products respectively. The increase of the initial (average) temperature T_o will decrease H(R) and increase both H(P) and the adiabatic temperature. Increasing T_o to T_{ig}, will decrease H(R) to zero and all of $\Delta H(T_{ig})$ will be available to be absorbed by the products [14,23].

Materials and Methods

Processing and synthesis

Used in the experiments Ni powder characteristics presented in table 1.

Table 1 – Nickel Powder Characteristics

Composition

C	Mn	Cu	Fe	S	Si	Ni
0.017	<0.01	<0.01	0.04	0.0002	0.31	Bal.

Size Distribution

Mesh Size	+100	+120	+140	+200	+270	+325	-325
Percent	4.2	3.0	6.1	15.2	15.9	13.7	41.9

Aluminum powder MERCK, max. particle size 125 micron, purity 99.5%.

Stoichiometric fractions of elemental powders to produce the NiAl phase (38.5wt%Ni + 61.5wt%Al) were mixed thoroughly and die-pressed at a pressure of 30 bars to form cylindrical compacts (diameter c. 15 mm and height c. 20 mm) of green density about 60% of theoretical. The cylindrical specimens were then pre-heated in a furnace where the exothermic reaction between the Ni and the Al particles initiates as soon as any area of the compact reaches the ignition temperature. In all of our experiments, the reaction was initiated at the top surface of the specimens after exposure to the furnace temperature for a period between 1 and 4 minutes, depending on pre-heating temperature. As the SHS combustion zone moves through the specimen, a series of reactions take place and the compact melts, since the combustion temperature (approaching 2000 °C is well above the melting temperature of the NiAl phase (1640 °C). Once the SHS reaction is completed, the specimen is removed from the furnace and air-cooled.

The microstructure of the NiAl product, its chemical homogeneity and its mechanical properties usually depend on the processing conditions as well as the compact geometry, because of their effect on the actual average compact temperature at the time of ignition and on the cooling rate of the NiAl melt. The dimensions and the initial density of the specimens were kept fixed, while the furnace temperature T_{fur} was varied from 700 to 1000°C. The time to reaction initiation t_{in} was not constant in the experiments but decreased with increasing the furnace temperature as the initiation temperature was reached quicker.

Characterization

The NiAl materials synthesized were characterized by a number of techniques including X-ray diffraction, optical and scanning electron microscopy, electron dispersive spectroscopy, and hardness testing.

Results and Discussion

Modelling of the compact temperature

The time to ignition t_{in}, defined as the period that the specimen remains inside the furnace until the reaction initiates depends upon the initial temperature of the furnace. The variation of t_{in} versus the furnace temperature T_{fur} as determined from the SHS experiments is shown in Figure 1.

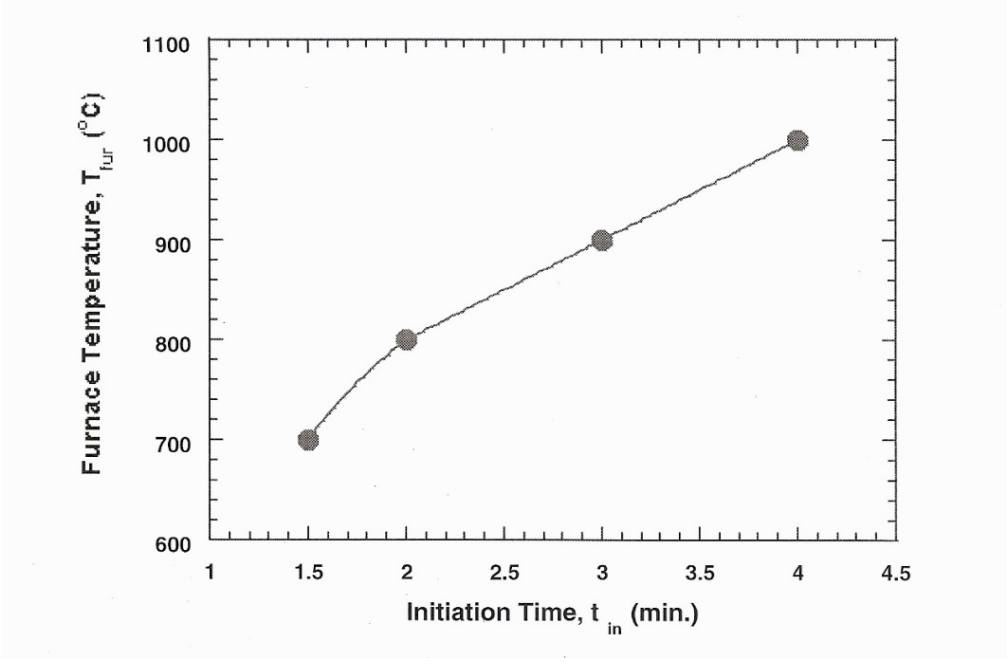

Figure 1 – The variation of initiation time t_{in} as a function of the furnace temperature T_{fur}

It is seen that as the furnace temperature increases the initiation time decreases because the ignition temperature (on the top surface of the sample) is reached faster. After ignition, the time required to propagate the reaction front along the specimen is less than 1 second, i.e. the reaction speed is quite high[1*]. Thus,

[1] *in fact, earlier work[16] on the synthesis of the 50% Ni – 50% Al system it was measured as being equal to XXX m/sec

with regard to the microstructure formation and evolution, it we accept that at the end of the reaction and prior to solidification, the material is at the liquid state. The microstructure obtained from the solidification process is dependent upon the difference between the temperature of the melt (which is related to the combustion temperature of the reaction) and the furnace temperature. Therefore, to interpret the microstructural features the combustion temperature (or likewise the average compact temperature) must be estimated.

As mentioned above in the section of "Thermodynamics", the maximum adiabatic temperature depends upon the average temperature of the compact. Evidently, the latter should be related to the furnace temperature and the time of exposure inside the furnace t_{in}. In order to gain a comparative estimate of the average compact temperature right before the reaction initiation for the various T_{fur} and t_{in}, a transient temperature analysis was conducted. In particular, the temperature at the center of the compact T_{cen} for the specific T_{fur} and t_{in} was calculated following the procedure which is outlined in the Appendix.

The variation of the temperature at the center of the compact versus the furnace temperature is shown in Figure 2.

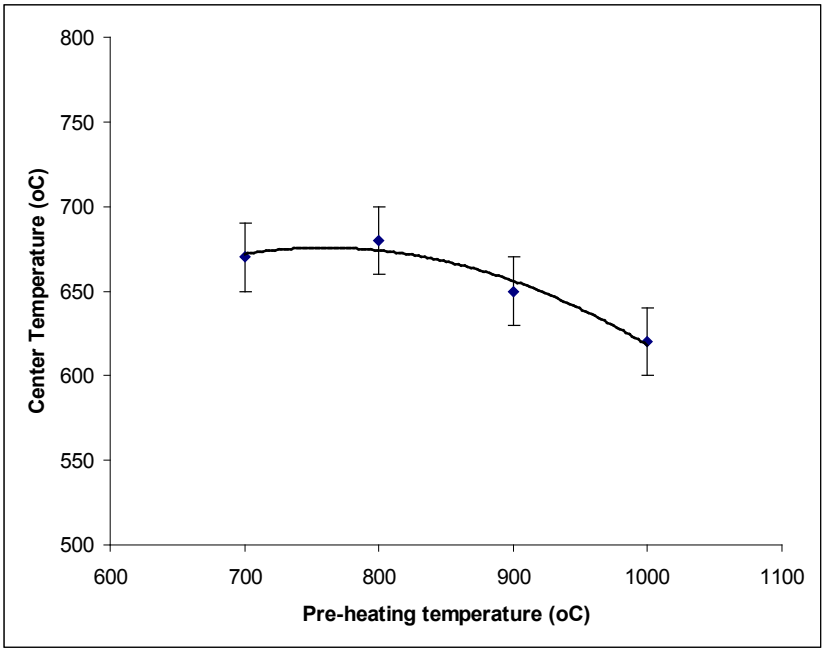

Figure 2 – The temperature at the center of the compact versus the furnace temperature

It is seen that, within the limits of the estimation error (which mainly arises from factors such as the accuracy of the calculation of the thermal properties of the porous compact) T_{cen} does not appear to vary with the furnace temperature. In other words T_{fur} and t_{in} are combined such that the temperature of the specimen's center has the same temperature irrespectively of the processing conditions. Therefore, since the temperature at the center of the specimen reflects its average temperature, it is deduced that the combustion temperature was the same for all of the experimental conditions. Given the fact that the ignition temperature (which in the experiments of this work was first reached on the top surface of the specimen) is dependent only upon the composition of the compact, the above analysis is important as it provides an indication that the average temperature of the specimen right before the ignition does not vary with the furnace temperature.

Characterization

a. X-ray Diffraction (XRD)

Figure 3 shows the XRD spectrum of a material fabricated by self-propagating synthesis of nickel and aluminum powder under the following processing conditions: furnace temperature 1000 °C, green compact density 60% of the theoretical, and initial dimensions 20 mm diameter and 15 mm height.

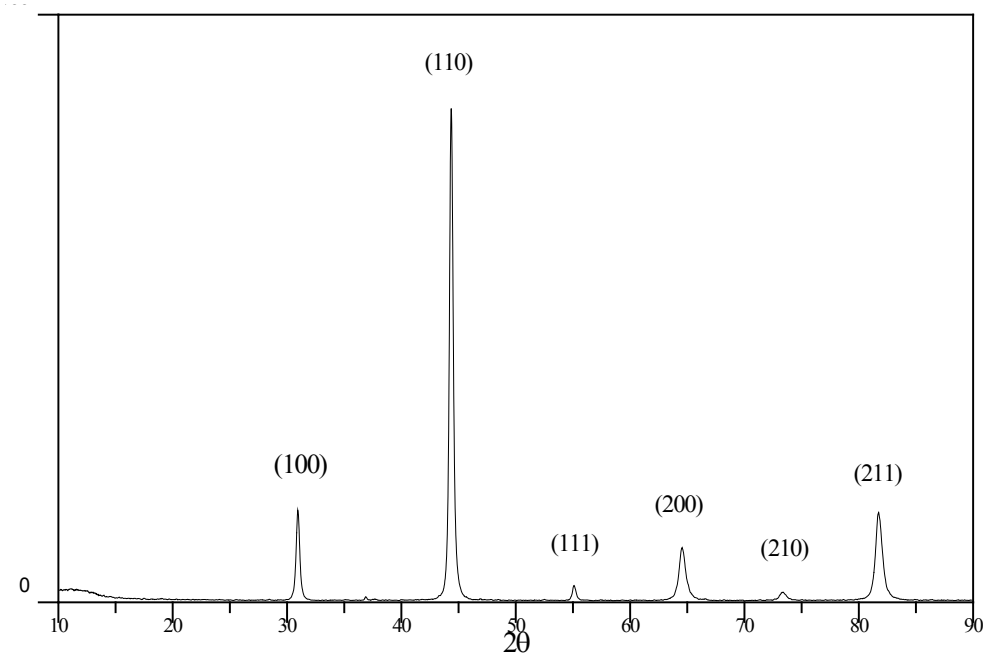

Figure 3 – Typical XRD spectra of NiAl produced by self-propagating high-temperature synthesis

In order to eliminate possible effects of the texture developed during the solidification of the melt, the specimen was pulverized, and its powder was used for the XRD characterization. All peaks that appear in the graph correspond to the NiAl intermetallic phase; no other intermediate phases between nickel and aluminum, or any oxides were detected, and no further elemental aluminum and nickel are present. In addition, materials synthesized under different processing conditions (i.e. furnace temperature, time exposed inside the furnace, etc.) were also examined by XRD, giving identical spectra to that shown in Figure 3. Therefore, in all cases pure monophase NiAl with the B2 ordered cubic structure with a lattice parameter α = 2.88Å was fabricated.

Earlier characterization work on the formation of NiAl compounds using differential thermal analysis (DTA) and synchroton radiation techniques revealed that during the SHS synthesis several intermediate phases such as Ni_3Al and Ni_3Al_2 are formed prior to the formation of the final, stoichiometric NiAl phase[23-24]. The formation as well as the presence of residues of the intermediate phases depends upon the combustion temperature. In particular, the proportion of the Ni_3Al and Ni_3Al_2 phases decreases as the combustion temperature increases. Therefore, the above results indicate that a high combustion temperature was achieved in our experiments.

Microstructure

As mentioned above, the NiAl formation proceeds through the formation of a melt. Examination of the microstructure at lower magnifications showed that the final product comprises two regions, a core which accounts for ~80% of the total volume of the compact. and a "shell" of high porosity (of the order of 20%) material around the core. This outer shell, whose microstructure is shown in Figure 4, owes its formation to the gravitational flow of a small portion of the liquid, since in our experiments the specimen stood free inside the furnace, thus flow of the melt was possible.

It is observed that the structure comprises large (~150 μm) grains of equiaxed shape. The fact that the NiAl grains have linear grain boundaries with no curvature indicate the high stability of the formed compound, the absence of secondary phases, and a very rapid crystallization of the primary melt. Although, no pores can be discerned from this micrograph; the higher magnification micrograph in Figure 6 shows that there are a few spherical with a size of less than 10 μm inside the material.

Although at low magnifications the microstructure of the core appears to be quite uniform, microstructural nonuniformities may be distinguished at higher magnifications. In particular, the SEM micrograph of Figure 6 reveals the presence of spherical particles within a fine grained matrix.

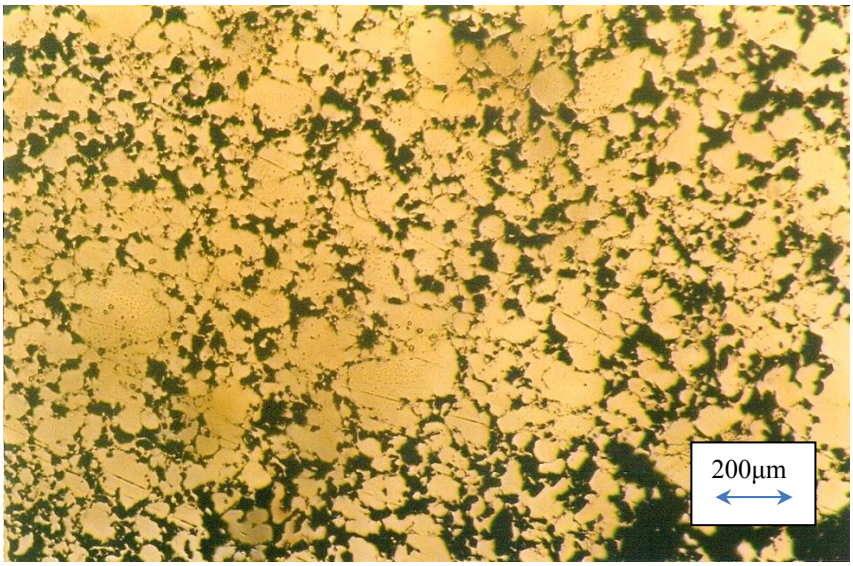

Figure 4 – Microstructure of NiAl-rich outer shell

A typical, low magnification, optical micrograph of the core is shown in Figure 5.

In conjunction with the XRD results it can be deduced that both the particles as well as the fine matrix are of pure NiAl. It is also seen that the pores are mainly located at the particle/matrix boundaries, which indicated that the large particles solidified first inside the matrix which was in the liquid state.

Hardness

The Vickers hardness of the NiAl compounds versus the furnace temperature at which they were synthesized is presented in Figure 8.

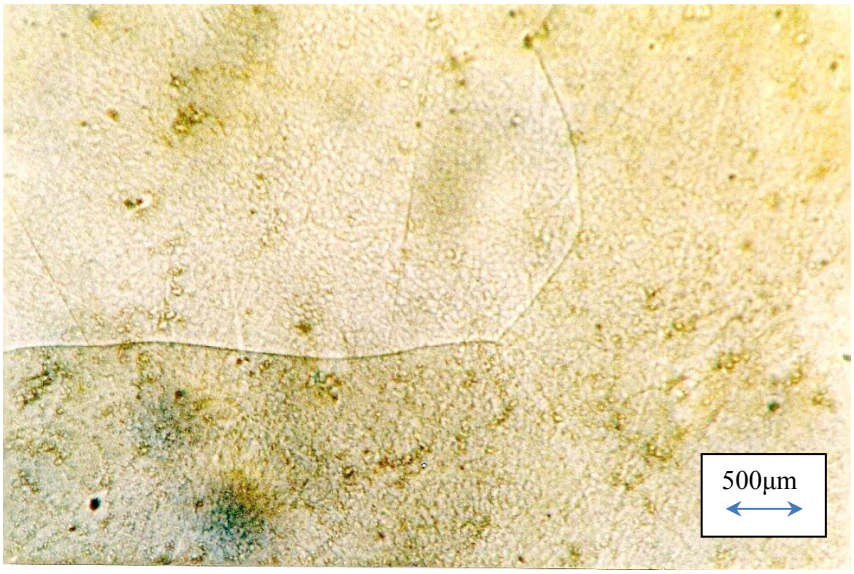

Figure 5 – Microstructure of the core

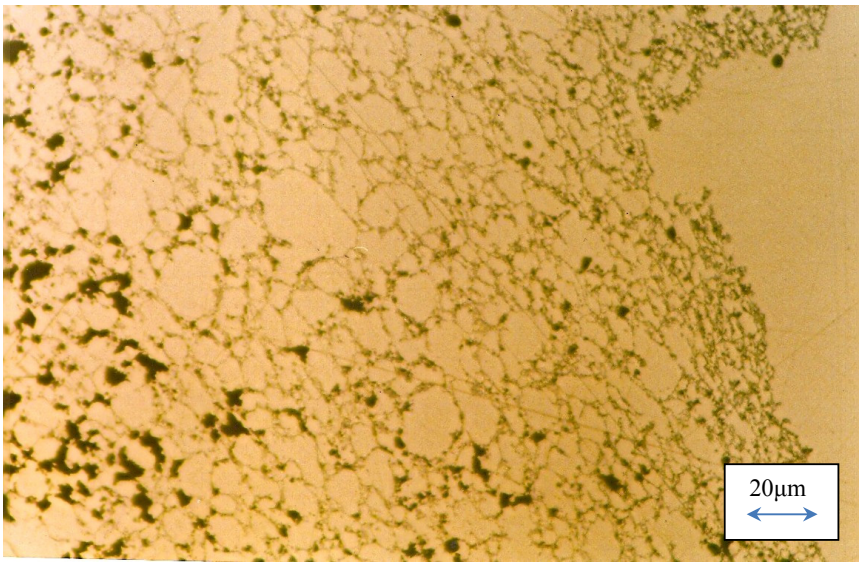

Figure 6 – Microstructure of semi-spherical particles within a fine grained matrix

The particles have a wide distribution of sizes ranging between 4 and 15 μm. The chemical composition of the particles as well as the composition of the matrix were determined by EDS analysis. The EDS spectra shown in Figure 7 do not reveal any essential differences on the peaks of nickel and aluminum between the particles and the matrix.

The results revealed a trend of decreasing hardness with increasing the furnace temperature. This hardness variation can be interpreted with regard to the cooling rate of the NiAl melt which is proportional to the difference ΔT between the temperature of the melt T_m and the temperature of the furnace T_{fur}. If it is assumed that the temperature of the melt is near the combustion temperature, (which as discussed in the previous sections is essentially constant for all conditions used) then ΔT increases as the furnace temperature decreases. Therefore, at lower T_{fur} the cooling rate is higher, resulting to a more brittle and harder microstructure. SEM micrographs of the fracture surface of NiAl compacts fabricated at furnace temperatures of 700 and 1000 °C are shown in Figures 9a and b respectively. The micrograph of Figure 9a shows a brittle type of fracture, while areas which have undergone plastic deformation are observed in Figure 9b. Interestingly, NiAl fibres were also found to have formed inside pores and are also visible in Figure 9a and b. This is the first time such fibres have been observed and the exact conditions of formation and characteristics are under investigation at present.

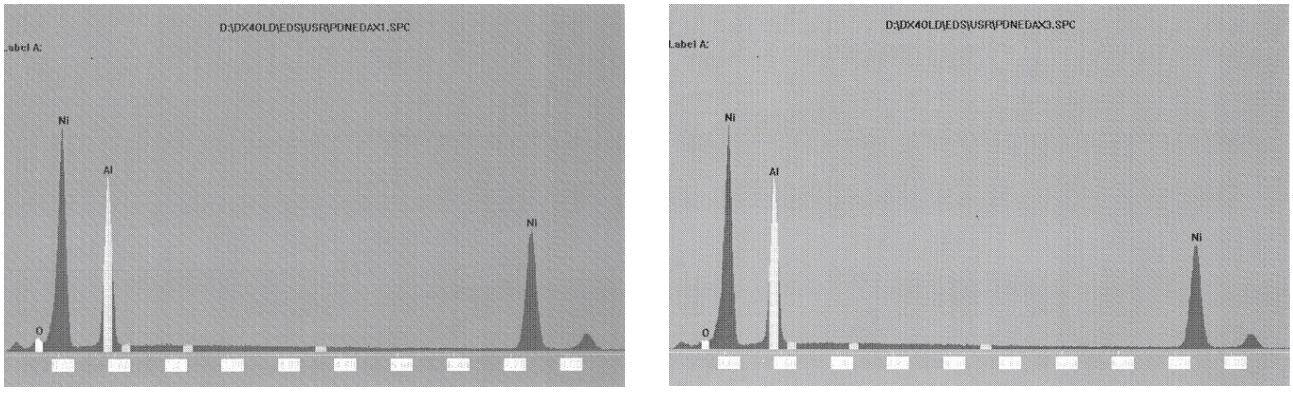

Figure 7 – The EDS spectra of the particles (left) and
the matrix (right) showing that they have almost identical elemental composition

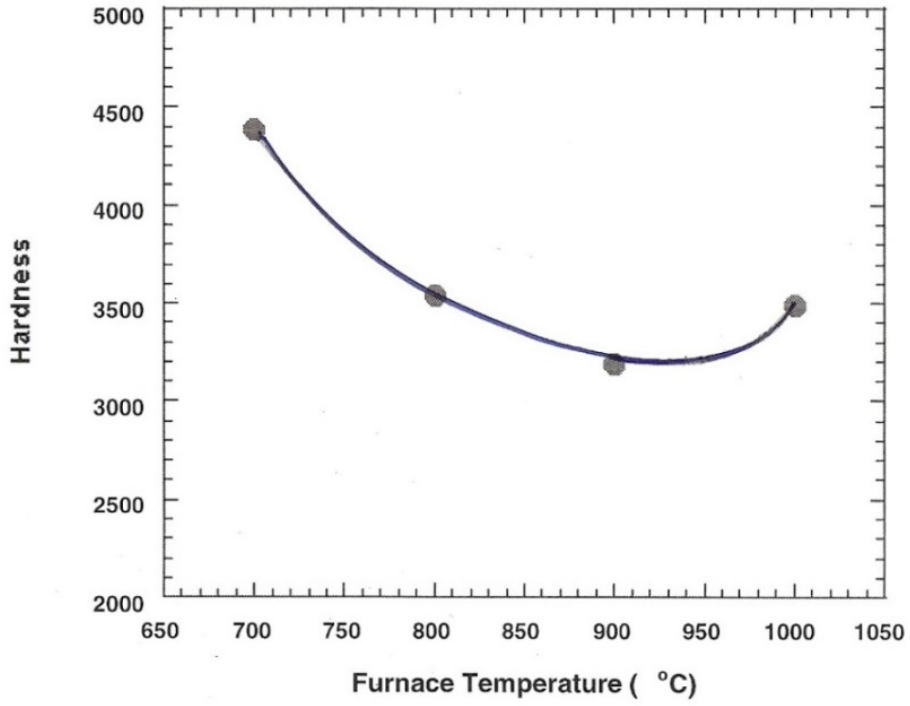

Figure 8 – The Vickers hardness of the NiAl compounds versus the furnace temperature.

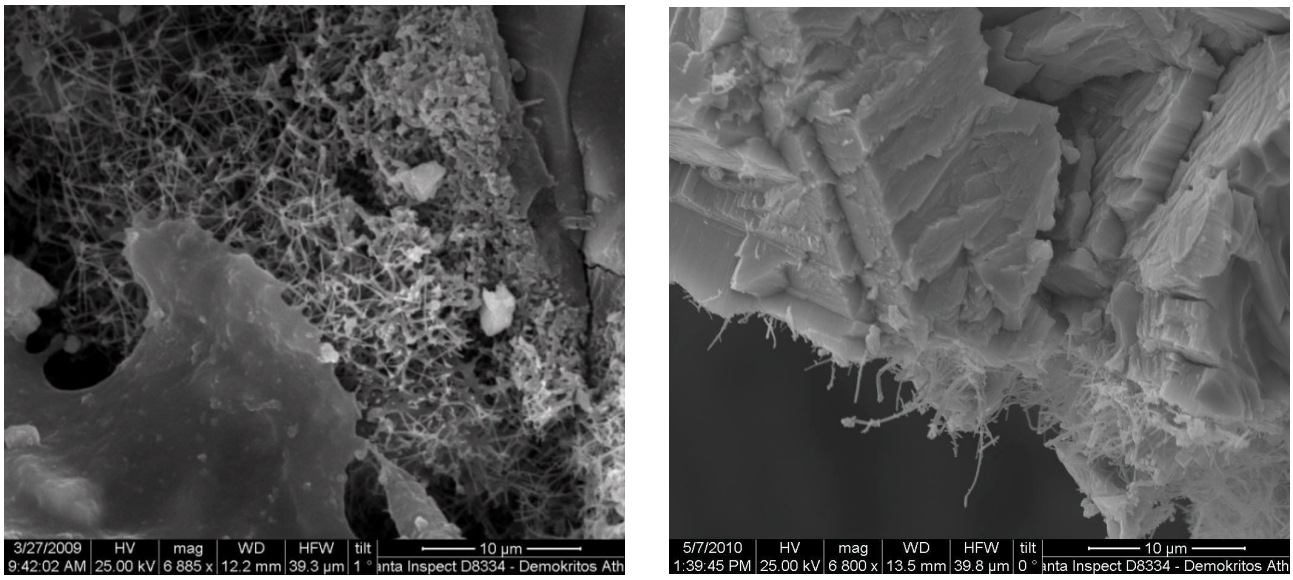

Figure 9 – SEM of SHS NiAi (initial mixture 60%Al- 40% Ni). Brittle fracture with some localized areas where limited plastic deformation are visible. NiAl fibres are also visible

In summary, the low sensitivity of the material hardness (and hence strength) upon the furnace temperature represents a significant technological advantage of the process from the industrial point of view, because it does not pose great difficulties in scale-up, and also the material quality does not vary greatly with the processing furnace temperature.

Summary and conclusions

The SHS method was used to synthesize the B2 NiAl compound from elemental nickel and aluminum powders. The main conclusions of this work may be summarized as follows:

1. X-ray diffraction showed that the NiAl is the only phase formed (through solidification of a melt) when the powder compacts are processed at a furnace temperature is at the 700-1000 ^{o}C range.

2. The microstructure consists of large equiaxed grains with linear grain boundaries. The latter indicate the high stability of the compound synthesized and a very rapid crystallization of the primary melt.

3. The hardness of the final product was fount to decrease with the increase of the furnace temperature because of the lower cooling rate of the melt.

4. The process used has shown that NiAl fibres can form inside pores of the material.

Ackowledgements

We'd like to thank Dr P. Nikolaou for his contribution in this work.

References

1. C.T. Liu and K.S. Kumar, Ordered Intermetallic Alloys, Part I: Nickel and Iron Aluminides, JOM, May 1993, pp. 38-41.

2. R.D. Noebe, R.R. Bowman, and M.V. Nathal, Review of the Physical and Mechanical Properties and Potential Applications of the B2 Compound NiAl, NASA Technical Memorandum 105598.

3. D.E. Alman, J.A. Hawk, A.V. Petty, and J.C. Rawers, "Processing Intermetallic Composites by Self-Propagating, High Temperature Synthesis", JOM, March 1994, 31-35.

4. A. Varma, C.R. Kachelmyer, and A.S. Rogachev, Mechanistic Studies in the Combustion Synthesis of Aluminides and Silicides, *Int. J. of Self. Prop. High-Temp. Synth.,* vol. 5, No 1, 1996, pp. 1-25.

5. T.S. Dyer and Z.A. Munir, The Synthesis of Nickel Aluminides by Multilayer Self-Propagating Combustion, *Metall. Mater. Trans. B,* vol. 26B, 1995, pp. 603-610.

6. Z.A. Munir, Reaction Synthesis Processes: Mechanisms and Characteristics, *Metall. Trans. A,* vol. 23A, 1992, pp. 7-13.

7. B. Michelic, M. Dakic, R. Djekic, and D. Uskokovic, Processing of Compact Materials by the Use of Self-Propagating High-Temperature Synthesis and Pseudo-Hot Isostatic Pressing, Mater. Lett., vol. 13, 1992, pp. 391-395.

8. H. Doty and R. Abbaschian, Reactive Hot Compaction of NiAl with in situ Alumina Reinforcement, mat. *Scie. Eng. A,* vol. A195, 1995, pp. 101-111.

9. J.J. Moore, D.W. Ready, H.J. Feng, K. Monroe, and B. Mishra, The Combustion Synthesis of Advanced Materials, JOM, November 1994, pp. 72-78.

10. D.E. Alman, C.P. Dogan, J.A. Hawk, and J.C. Rawers, Processing, Structure and Properties of Metal-Intermetallic Layer Composites, *Mater. Scie. Eng. A,* vol. A192/193, 1995, pp. 624-632.

11. Z.P. Xing, J.T. Guo, G.Y. An, and Z.Q. Hu, Hot Pressing Aided Exothermic Synthesis and Densification of NiAl and NiAl-TiC Composite, *Int. J. of Self. Prop. High-Temp. Synth.,* vol. 5, No 1, 1996, pp. 51-56.

12. A.G. Merzhanov, Worldwide Evolution and Present Status of SHS as a Branch of Modern R&D, *Int. J. of Self. Prop. High-Temp. Synth.,* vol. 6, No 2, 1997, pp. 119-163.

13. 15. J.J. Moore and H.J. Feng, Combustion Synthesis of Advanced Materials: Part II.Classification, Applications and Modeling, Prog. Mater. Scie., vol. 39, 1995, pp. 274-316.

14. Z.A. Munir, Synthesis of High Temperature Materials by Self-Propagating Combustion Methods *Ceram. Bull.,* vol. 67, No 2, 1988, pp. 342-349.

15. Shushan Dong, Ping Hou, Haiyong Cheng, Haibin Yang and Guangtian Zou, Fabrication of intermetallic NiAl by self-propagating high-temperature synthesis reaction using aluminium nanopowder under high pressure, 2002 *J. Phys. Condens. Matter* 14 11023

16. Effects of TiC addition on combustion synthesis of NiAl in SHS mode YEH C. L., SU S. H., CHANG H. Y., *Journal of alloys and compounds* 2005, vol. 398, pp. 85-93

17. Iris V. Rivero, Michelle L. Pantoya, Karthik Rajamani, Simon M. Hsiang, Correlation of reactant particle size on residual stresses of nanostructured NiAl generated by self-propagating high-temperature synthesis *Materials Research Society,* v.24, n.6, pp. 2079- 2088

18. Roy, S. K. and Biswas, A'Combustion of Powder Mixtures Forming Reaction Products -Synthesis of NiAl', *Mineral Processing and Extractive Metallurgy Review,* 22: 2, 567 – 596.(2001)

19. D. Tingaud, L. Stuppfler, S. Paris, D. Vrel, F. Bernard, C. Penot and F. Nardou, Time-resolved X-ray diffraction study of SHS-produced NiAl and NiAl-ZrO_2 composites *Int.Journal SHS, 2007,* Volume 16, Number 1, Pages 12-17

20. V. I. Vershinnikov and I. P. Borovinskaya, Fine TiAl and NiAl powders by SHS with a reduction stage *Int. Journal SHS,* 2009, Volume 18, Number 2, Pages 97-101

21. A. Biswas , S.K. Roy, Comparison between the microstructural evolutions of two modesof SHS of NiAl: key to a common reaction mechanism, *Acta Materialia* 52 (2004) 257–270

22. A. Shchukin, D. Vrel, A. Sytschev, Interaction of NiAl Intermetallic During SHS Synthesis with Ta Substrate, February 2018, Advanced Engineering Materials DOI: 10.1002/adem.201701077

23. J.J. Moore and H.J. Feng, Combustion Synthesis of Advanced Materials: Part I. Reaction Parameters, *Prog. Mater. Scie.,* vol. 39, 1995, pp. 243-273.

24. M.C. Dumez, R.M. Marin-Ayral, and J.C. Tedenac, La Synthese Auto-Propagee Haute Pression Appliquee aux Intermetalliques de Type Nickel-Aluminum, *Mater. Res. Bull.* vol. 29, No 6, 1994, pp. 611-617.

25. A.V. Luikov, A.G. Slskov, L.L. Vasiliev, and Y.E. Fraiman, *Int. J/ Heat Mass Transf.,* vol. 11, pp. 117-125, 1968

26. W.D. Kingery, H.K. Bowen, and D.R. Uhlmann, Introduction to Ceramics, 2nd Edition, J. Wiley & Sons, New York, 1976.

27. A.D. Brailsford and K.G. Major, Br. *J. Appl. Phys.,* vol. 15, 1964, pp. 313-320.

28. G.H. Geiger and D.R. Poirier, Transport Phenomena in Metallurgy, Addison-Wesley Publishing Co, Reading MA, 1973.

29. F. P. Incropera and D.P. DeWitt, Fundamentals of Heat and Mass Transfer, 2nd Edition, J. Wiley & Sons, New York, 1985

30. D. Tingaud, L. Stuppfler, S. Paris, D. Vrel, F. Bernard, C. Penot and F. Nardou, Time-resolved X-ray diffraction study of SHS-produced NiAl and NiAl-ZrO_2 composites, *Int. Journal SHS,* 2007, Volume 16, Number 1, Pages 12-17

31. V. I. Vershinnikov and I. P. Borovinskaya, Fine TiAl and NiAl powders by SHS with a reduction stage *Int. Journal SHS,* 2009, Volume 18, Number 2, Pages 97-101

32. A. Biswas, S.K. Roy, Comparison between the microstructural evolutions of two modesof SHS of NiAl: key to a common reaction mechanism, *Acta Materialia* 52 (2004) 257–270

33. A. Shchukin, D. Vrel, A. Sytschev, Interaction of NiAl Intermetallic During SHS Synthesis with Ta Substrate, February 2018, Advanced Engineering Materials DOI: 10.1002/adem.201701077